2015-07-03

Evidence of High Electrocatalytic Activity of Molybdenum Carbide Supported Platinum Nanorafts

Elbaz, Lior

Elbaz, Lior, et al. "Evidence of High Electrocatalytic Activity of Molybdenum Carbide Supported Platinum Nanorafts." Journal of The Electrochemical Society 162.9 (2015): H681-H685.

Journal of The Electrochemical Society, **162** (9) H681-H685 (2015)
0013-4651/2015/162(9)/H681/5/$33.00 © The Electrochemical Society

Evidence of High Electrocatalytic Activity of Molybdenum Carbide Supported Platinum Nanorafts

Lior Elbaz,[a,z] Jonathan Phillips,[b] Kateryna Artyushkova,[c,*] Karren More,[d,*] and Eric L. Brosha[e,*]

[a]*Department of Chemistry, Bar-Ilan University, Ramat Gan 52900, Israel*
[b]*Naval Post-Graduate School, Monterey, California 93943, USA*
[c]*Department of Chemical Engineering, University of New Mexico, Albuquerque, New Mexico 87131, USA*
[d]*Materials Science and Technology Division, Oakridge National Laboratory, Oak Ridge, Tennessee 37831, USA*
[e]*Materials Physics and Applications Division, Los Alamos National Laboratory, Los Alamos, New Mexico 87545, USA*

A remarkable new supported metal catalyst structure on Mo_2C substrates, 'rafts' of platinum consisting of less than 6 atoms, was synthesized and found to be catalytically active electrocatalyst for oxygen reduction. A novel catalytic synthesis method: Reduction-Expansion-Synthesis of Catalysts (RES-C), from rapid heating of dry mixture of solid precursors of molybdenum, platinum and urea in an inert gas environment, led to the creation of unique platinum Nanorafts on Mo_2C. The Pt Nanorafts offer a complete utilization of the Pt atoms for electrocatalysis with no "hidden" atoms. This structure is strongly affected by its interaction with the substrate as was observed by XPS. In this work, we show for the first time, evidence of electrocatalytic activity with such small clusters of non-crystalline Pt atoms as catalysts for oxygen reduction. Electrochemical half-cell characterization shows that this structure permit more efficient utilization of platinum, with mass activity conservatively measured to be 50% that of platinum particles generated using traditional approaches. Moreover, as cathode fuel cell catalysts, these novel material may dramatically enhance stability, relative to the commercial Pt/carbon catalysts.

Manuscript submitted May 19, 2015; revised manuscript received June 16, 2015. Published July 3, 2015. This was Paper 614 presented at the Orlando, Florida, Meeting of the Society, May 11–15, 2014.

Fuel cell technology, specifically proton exchange membrane fuel cell (PEMFC), potentially can economically replace combustion engines for transport, with high efficiency, clean (water–only) energy. The US department of energy (DOE) identifies two remaining major hurdles to the deployment of this alternative: cost and durability of the cathode.[1] Reducing the amount of platinum, will help overcome the first problem. In addition, creation of a new, 'non-carbon', more oxidation resistant catalyst support material could potentially overcome the second difficulty. Here, we describe a new technology that significantly advances both objectives.

Platinum, still the best catalysts for oxygen reduction reaction (ORR) in fuel cells[2] was used in core-shell structures[3] and alloyed with transition metals[4] in order to reduce its loading. In most cases, significant reduction was obtained with increased activity, attributed to the interaction between the Pt and non-Pt atoms in the catalyst. M. Nesselberger et al. showed that it is possible to obtain very active Pt-based catalysts when forming small nano clusters of Pt on carbon, and measured activity that is 6 times higher than commercial Pt on carbon.[5] In a different study, Qiao et al. showed an unprecedented CO oxidation catalytic activity of a single atom of Pt on FeO_x which was attributed to the interaction between the Pt atoms and the FeO_x.[6]

At present, carbon is the preferred catalyst support, because it has the primary features required: abundant, high surface area and good electrical conductivity. However, the use of carbon is clearly problematic. The conditions in PEMFCs are oxidizing, especially in the cathode.[7–9] These conditions are detrimental to the carbon and the catalysts which interact with it and shorten the lifetime of PEMFCs.[10,11] For these reasons, alternative supports have been developed, mainly electronically conductive ceramic supports such as titanium oxides,[12,13] molybdenum nitride,[14] and tungsten oxide.[15] In the present work we continue this endeavor, with yet another conductive material: molybdenum carbide. Although some preliminary work has been done, mainly as a catalyst support for the anode,[16–19] the performance and durability of this material as a catalyst support in oxidizing environment in a PEMFC cathode has not been extensively studied.

There are several techniques for the synthesis of molybdenum carbide, the most common of which is the temperature programmed reaction (TPR) of various molybdenum precursors in carbonaceous gas atmospheres.[20] This synthesis results in free carbon left in the Mo_2C as an impurity. The properties of the resulting molybdenum carbide phase and the carbon content were found to be dependent on the reactant gas composition and the temperature.[20–23] In a previous work[24] we reported the synthesis of molybdenum carbide using the polymer assisted deposition (PAD) method developed by Jia et al.,[25] which yielded ~40%$_{wt}$ of amorphous carbon. It was also shown that, when added to molybdenum carbide supports, Pt shows higher mass activity and lower overpotential for oxygen reduction reaction (ORR) electrocatalysis.

In addition to a more detailed exploration of Mo_2C as a support, we also report on improvements created simply by the use of a different synthesis protocol. That is, the Pt Nanorafts catalysts (nominally 5% Pt on Mo_2C) produced by the novel RES-C method are not chemically different than those produced using standard synthesis, yet the morphology of the Nanoraft catalysts is unique. In this technique, Pt is imbedded in the support during the support synthesis, and not subsequent to synthesis, as per all other catalyst synthesis techniques. There are several possible advantages in incorporating the catalyst in the support during its synthesis: 1) the support is not yet exposed to outside environment which can result in partial oxidation of the surface and introduce impurities that may act as poisons, 2) the adhesion of the catalysts to the support is expected to be stronger, and, 3) the process is simplified and reduced to the minimum necessary synthesis stages.

Experimental

Nanorafts Synthesis using the RES-C method: Each 1.0 g of 5 wt% Pt/Mo_2C catalyst was generated from the following weights of three (all obtained from Sigma Aldrich, >99% purity) reagents: 0.1 g of tetra-amine platinum nitrate ($(NH_3)_4Pt(NO_3)_2$), 0.6 g of urea and 1.78 g of ammonia molybdate $(NH_4)_6Mo_7O_{24}{\cdot}4H_2O$). These reagents were mixed in two stages using a small metal blade 'food processor' (volume ~200cc). First, the tetra-amine platinum nitrate and urea were blended for approximately 10 seconds, and the homogenized mixture left in the blender. Second, ammonia molybdate was added to the mixture in the blender, and all mixed for approximately 30 seconds. This three component (urea, tera-amine platinum nitrate and ammonia molybdate) homogenized mixture created by the mixing process was placed in a ~20 ml alumina boat. The boat was maneuvered to the center of a 2.5 cm diameter by 30 cm length quartz tube attached

*Electrochemical Society Active Member.
[z]E-mail: lior.elbaz@hotmail.com

to a gas handling system. The tube was continuously flushed with nitrogen gas (> 8 flushes by volume). Once the flushing was judged to have removed of the order 99% of the oxygen originally present, the tube, still continuously flushed with nitrogen, but at a very slow rate (ca. estimated gas velocity 0.1 cm/sec), was placed inside a tube furnace pre-heated to 800°C. After 300 seconds the tube was removed from the furnace, the nitrogen flow rate dramatically increased. After the tube was thoroughly cooled the material in the alumina boat was removed for characterization and catalyst testing.

High-resolution transmission electron microscopy (HR-TEM) images were collected using an aberration-corrected JEOL 2200FS microscope. High angle, annular dark field (HAADF) scanning transmission electron microscopy (STEM) images were acquired with a convergence angle of 27 mrad and an inner collection angle of 100 mrad.

X-ray photoelectron spectroscopy (XPS) was performed on a Kratos Axis DLD Ultra X-ray photoelectron spectrometer. Spectra were recorded under the operating pressure of around 2×10^{-9} Torr using a monochromatic Al K_α source operating at 300 W with no charge compensation. Low energy resolution survey-range spectra were acquired at 80 eV pass energy while high resolution spectra were acquired at a pass energy of 20 eV. Quantification of XPS was performed using Casa XPS software. Curve-fitting was carried out using individual peaks with 70% Gaussian/30% Lorentzian line shape.

XRD measurements were performed using a Siemens D5000 powder x-ray diffractometer using CuK_α radiation and an incident beam, graphite monochrometer. Full profile fitting of the collected data was performed using MDI Shadow software package.

Trace element analysis was used to measure the loading of platinum in the molybdenum carbide-carbon using a SpectraceQuanX X-ray fluorescence (XRF) spectrometer. A Fundamental Para-meters model (NIST) and pure element standards were used to determine metal concentrations.

Electrochemical experiments were performed in order to study the catalysis of ORR with Nanorafts and compare it to commercially available Pt based catalyst for PEMFCs. All experiments were conducted in oxygen saturated 0.1 M $HClO_4$ (dissolved in deionized water) in a half cell configuration, and all the results are reported in reference to a real hydrogen electrode (RHE). Rotating ring-disk electrode (RRDE) was used to evaluate the ORR catalytic activity and compare it to commercially available platinum supported on carbon: 5%$_{wt}$ Pt on XC-72. Accelerated stress tests were conducted in half cell under Ar by cycling between 0.6 to 1.3 V vs. RHE and measuring the electro-active surface area (ECSA) of the Pt.

Results and Discussion

Two types of cubic phase molybdenum carbide, Mo_2C were synthesized: one devoid of Pt in which only the Mo_2C support was synthesized, and one Mo_2C support sample synthesized with a source of Pt that result in Pt Nanorafts. A third catalyst sample comprised of Pt deposited on the Pt-free Mo_2C via incipient wetness technique[13] was prepared and this served as an empirical comparison of performance between the sample with imbedded Pt and one with Pt disposition conducted using methods common to the preparation of Pt/C fuel cell catalysts.

X-ray diffraction (XRD) shows clear differences in the structure of the three samples. The XRD trace of the molybdenum carbide only material (Figure 1a) shows a non-stoichiometric Mo_2C_{1-n} pattern. Moreover, the appearance of the peak at 49° is an indication that sufficient non-stoichiometry is obtained in the sample such that it is no longer of cubic symmetry. Figure 1b shows the molybdenum carbide support after disposition of 5%$_{wt}$ Pt using an incipient wetness approach. Here the Pt is clearly present with strong diffraction peaks at 40°, 46°, 68°, 82° and 86° two-theta. The average crystallite sizes were obtained using simultaneous full-profile fitting of these data, and were found to be of 23Å and 54Å for the carbide and Pt phases respectively. In comparison, the Pt Nanorafts shows no diffraction intensity from the Pt phase, suggesting a high dispersion of Pt was

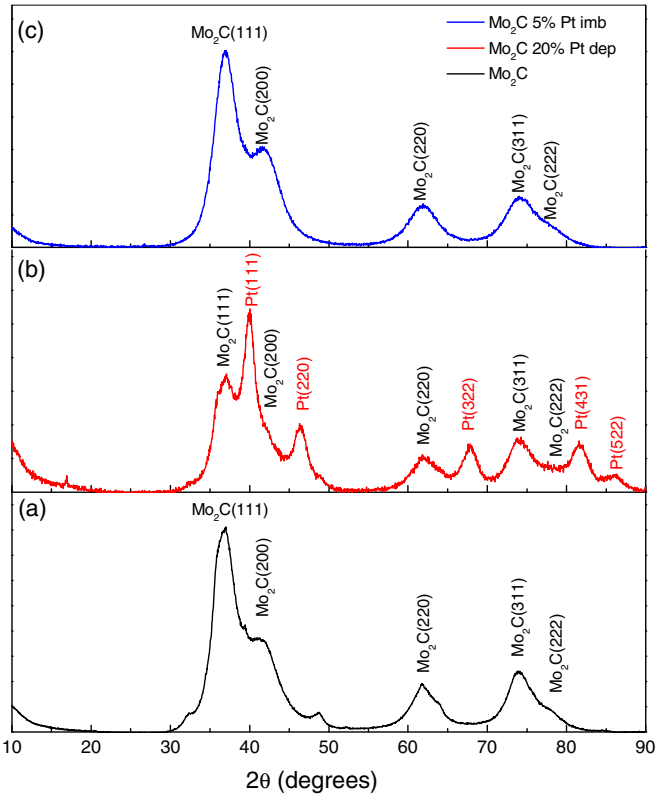

Figure 1. XRD of (a) Mo_2C, (b) Platinum deposited on Mo_2C and (c) Pt Nanorafts.

achieved throughout the sample, or that the Pt is present in very small clusters (<1 nm). The presence of only diffraction peaks related to a cubic symmetry suggests that the bulk of this sample is close to stoichiometry.

Since Pt features were not observed in the XRD traces of samples when the Pt was imbedded in the Mo_2C during the synthesis of the support (Fig. 1c), the presence of Pt in Nanoraft sample was confirmed using XRF and found to be 4.8%$_{wt}$, close to the nominal 5%, with a Fundamental Parameters method and pure Pt and Mo_2C as calibration standards.

Transmission electron microscope (TEM) was used to further characterize the Pt Nanorafts. The sample was composed of two agglomerate morphologies (1) spongy-porous and (2) sheet-like (Fig. 2).

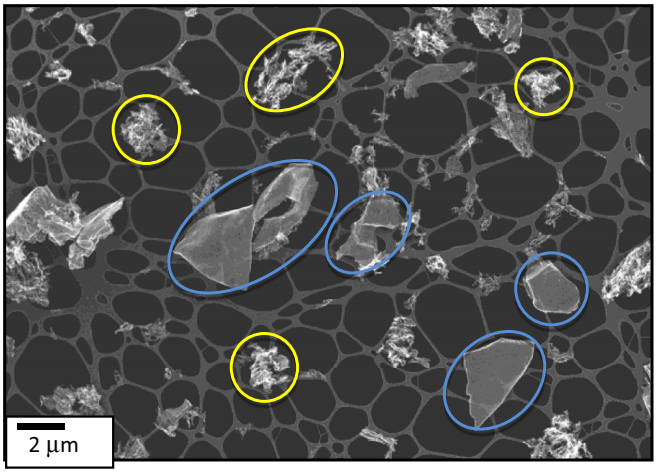

Figure 2. TEM images of Pt Nanorafts showing (1) spongy-porous (yellow) and (2) sheet-like (blue) morphologies.

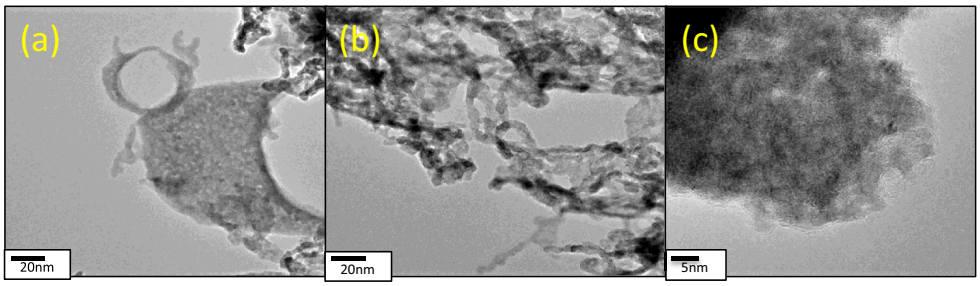

Figure 3. TEM images of (a) Sheets of nano-crystalline Mo_2C, (b) Nanowire of nano-crystalline Mo_2C and (c) Large sheet of densely packed Mo_2C.

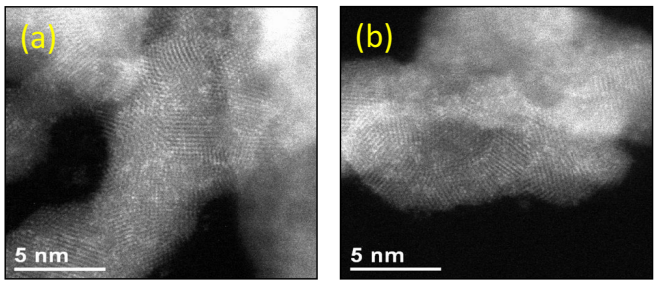

Figure 4. High-angle annular dark field (HAADF) STEM images of Pt imbedded Mo_2C.

The spongy-porous agglomerates are comprised of a 'skeleton' of nano-crystalline Mo_2C that forms interlocking flat-sheets (Fig. 3a) and nano-wires (Fig. 3b) and large sheets (Fig. 3c) that are thin and comprised of densely packed nano-crystalline Mo_2C. As it seems, the sheets originate from the spongy-porous material and were detached from the connecting nano-wires and non-crystalline Mo_2C during the synthesis. The Pt is homogenously dispersed throughout the Mo_2C support and could be seen in the high-angle annular dark field (HAADF) STEM image (Fig. 4), where the brighter "islands" distributed on the Mo_2C surface are small clusters of Pt atoms. These Nanorafts are composed of three to six atoms of Pt. These structures are not Pt nano-particles and are not crystalline. This supports the previous observation made using XRD, where Pt was not detected once it was imbedded in the Mo_2C.

The electronic interaction between the platinum Nanorafts and the surface of the Mo_2C support were studied using X-ray photoelectron spectroscopy (XPS). These results were compared to those obtained with commercially available electrocatalyst: $20\%_{wt}$ platinum on carbon XC-72. Figure 5 shows Pt 4f and C 1s spectra for Pt Nanorafts on Mo_2C and for Pt on XC72.

This data reveal that the electronic structure of platinum is significantly impacted by the Mo_2C support. The Pt 4f peak for commercial Pt on carbon (XC-72) mainly has three types of Pt present: metallic Pt (the dominant type of Pt), Pt associated with carbon and some oxidized Pt at the highest binding energy. In contrast, on Mo_2C, the 4f peak shows most of the Pt is associated with the carbon from the molybdenum carbide. This is not Pt carbide, as there is no peak at 71.1 eV where one would expect to observe the Pt carbide peak. On Mo_2C, the bond between Pt and C is of the complexing type generally associated with organometallic compounds.

In the C 1s spectrum for Pt on XC-72 the peak at 284.3 eV is the most dominant. This peak is attributed to graphitic carbon. The interpretation of this peak as arising from graphite is consistent with shake-up peaks in the higher BE region (>290 eV). In contrast, there are no shake-up peaks detected for the Mo_2C sample suggesting that

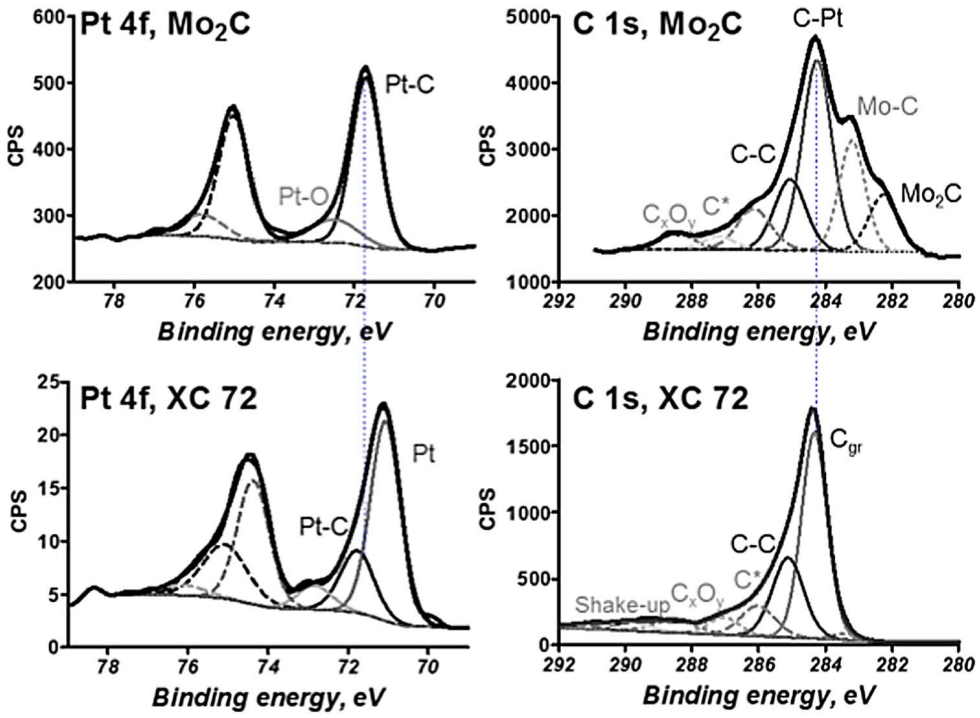

Figure 5. High resolution XPS Pt 4f and C 1s spectra for Pt on Mo_2C and Pt on carbon (XC72).

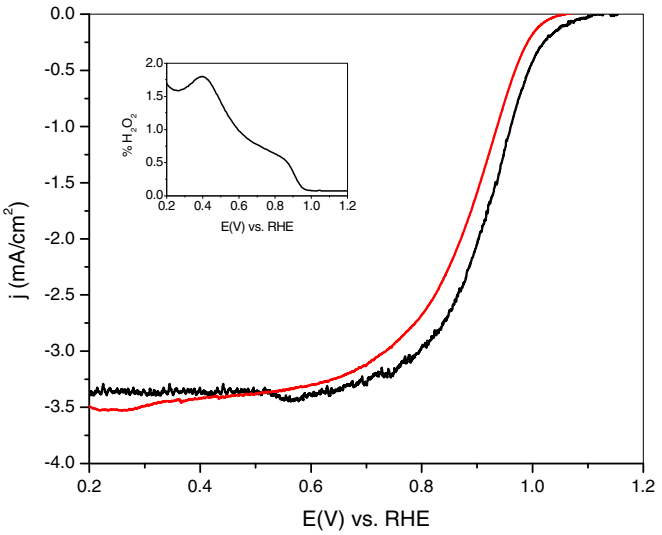

Figure 6. RDE at 900 rpm and 5 mV/s in oxygen saturated 0.1 M $HClO_4$ in DI water of 5% Pt/XC72 (red line) and Nanorafts (5% Pt on Mo_2C) (black line).

peak at 284.3 eV is possibly due to Pt-C complexing bond on carbon associated with the Mo_2C.[26]

On XC-72, 23% of the Pt is bound to a mixture of graphitic and amorphous carbon. There are sufficient reports in the literature of durability studies undertaken that suggest this bond is weak and allows platinum to migrate and sinter.[27] In contrast, as confirmed here by XPS, for these Pt Nanoraft structures prepared on Mo_2C, we found no evidence of 'free' Pt that is not interacting with the support. Thus, we would argue that all of the Pt on Mo_2C in this material is potentially stabilized against sintering due to interaction between platinum and carbon in the support.

Electrochemical Performance

Suspensions of Nanorafts and a commercially available Pt/XC-72 in 0.05%$_{wt}$ Nafion in isopropanol were prepared and 30 µl were deposited on the glassy carbon disk of an RRDE electrode and were to let dry overnight. Figure 6 shows the RDE results obtained with Nanorafts and Pt/XC-72 at 900 rpm and 5 mV s^{-1}. From these results, the half wave potential for ORR with Nanorafts is 0.92 V vs. RHE, whereas with the carbon supported Pt, the measured half wave potential is 0.89 V vs. RHE.

A difference in onset potentials was also observed and was found to be 1.11 V and 1.04 V vs. RHE for the Nanorafts and Pt/XC-72, respectively. The reaction seems to be predominantly a four electron reduction of oxygen to water in both cases, as insignificant amounts (less than 2%) of peroxide were formed and detected by the Pt ring on the RRDE electrode (Fig. 6 inset). The limiting current correlates to a 3.6 electron process according to the value obtained from the Levich equation:

$$i_{\mathrm{Lev}} = 0.62nFAD^{2/3}\omega^{1/2}\nu^{-1/6}C^*_{\mathrm{O_2}}$$

Where A is the electrode area (cm^2), D and C are the oxygen diffusion coefficient (cm^2 s^{-1}) and bulk concentration (mol L^{-1}), respectively, ν is the kinematic viscosity of the solution (cm^2 s^{-1}) and ω is the angular frequency of rotation ($\omega = 2\pi f/60$, f is the disk rotation rate (rpm)). This is in agreement with the peroxide detected on the ring. Tafel plot was constructed from the RDE data of the Pt Nanorafts. The plot is divided into two sections, one with a slope of −60 mV/decade and the other with a slope of −126 mV/decade, very similar to the slopes obtained with crystalline Pt on carbon supports, indicating similar ORR mechanism.[28] The ORR transfer coefficient and exchange current density were calculated from the linear fitting to Figure 7 (for the Tafel

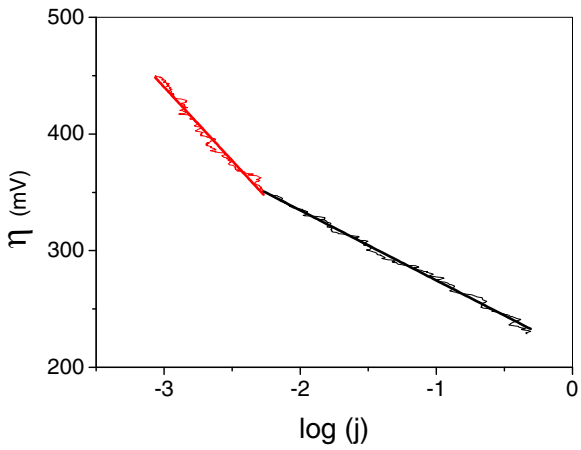

Figure 7. Tafel plot for ORR with Pt Nanorafts.

slope of −126 mV/decade). They were found to be equal to 0.47 and 8.99 µA/cm^2, respectively. The exchange current density measured with the Pt Nanorafts is one of the highest recorded with Pt-based catalysts, and is attributed to the interaction of the Pt atoms to the molybdenum carbide as also suggested by the XPS measurements.[29]

The activity per mass unit of Pt was calculated from the RRDE data according to the following equation:

$$i_{mass} = \frac{i_L \times i}{(i_L - i) \times m_{pt}}$$

Where i_{mass} is the mass activity (A g_{pt}^{-1}), i_L and i are the limiting current and current measured in RDE experiments (A) and m_{Pt} is the total mass of Pt on the electrode (g). The mass activity of the Nanorafts and Pt/XC-72 was plotted versus the potential (Fig. 8). It is apparent from these data that the Nanorafts are superior to the commercially available platinum on carbon per mass unit as the mass activity of the Nanorafts reaches 290 A g_{Pt}^{-1} whereas the Pt/XC-72 is only 190 A g_{Pt}^{-1} at 0.9 V vs. RHE. These results may be interpreted in two fashions. One: the utilization of the Pt in the Nanorafts is higher than on nano-crystals of Pt on carbon, due to the simple sheet-like morphology of the rafts, which leaves all Pt atoms exposed (100% dispersion). In contrast, the theoretically accessible percentage of Pt atoms on carbon is not more than 25% (the available Pt atoms in a 2 nm FCC Pt crystallite; from a simple calculation). Two: In a theoretical calculation we made in a previous publication, we showed

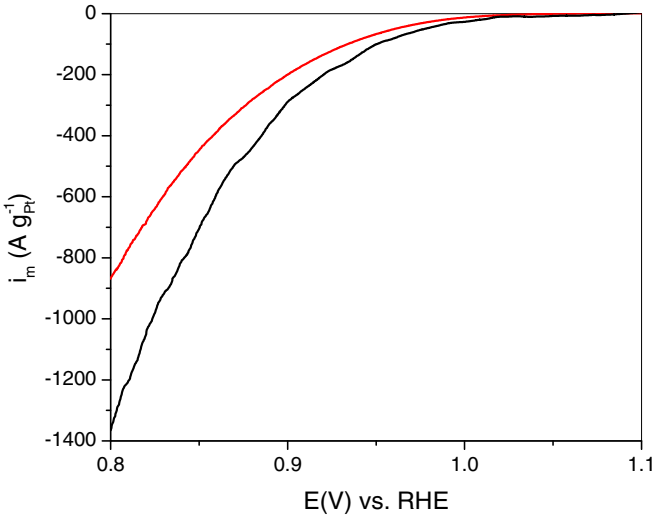

Figure 8. Mass activity calculated of Pt NanoRafts (black line) and Pt/XC-72 (red line). Inset: peroxide yield from ORR on the Nanorafts.

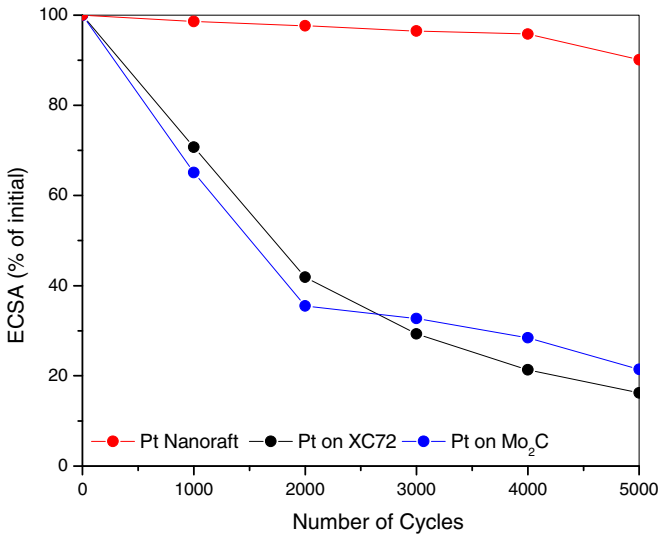

Figure 9. Accelerated stress tests of commercial Pt/XC-72 catalyst (black), Pt deposited via incipient wetness on Mo_2C (blue) and Nanorafts on Mo_2C (red).

that due to the interaction between Pt and Mo_2C, the binding of the Pt atoms to the surface of Mo_2C is stronger than Pt on a Pt(111) surface. Moreover, due to this electronic interaction, the surface Pt is prone to show better electrocatalytic activity towards ORR when compared to Pt on carbon (XC-72).[24]

In order to ascertain how well these Pt Nanorafts can withstand corrosion induced by PEMFC operation and resist activity losses do the Pt dissolution and coalescence,[30] we tested this material using a half-cell, accelerated stress test (AST), as described in the Experimental section, and compared the results to a commercial Pt/XC-72 fuel cell catalyst, and to the Pt/Mo_2C catalyst made using the traditional incipient wetness approach.

It is apparent from Figure 9 that there is a significant difference in the durability of the Mo_2C supported Nanorafts, crystalline Pt deposited on Mo_2C and the industry standard fuel cell catalyst, Pt on XC-72. Only 10% of the electrochemical surface area (ECSA), a measure of its availability for electrocatalysis, of the Nanorafts was lost after 5000 cycles, whereas Pt deposited on both Mo_2C and

XC-72 exhibited similar performance and lost around 80% of its ECSA. It is postulated that the phenomenal durability exhibited by the Nanorafts is due to strong binding to the Mo_2C surface. This will be the case of a future theoretical study of Pt Nanoraft.

Conclusions

In this work the unique morphology, surface bonding and catalytic activity of Pt/Mo_2C catalysts synthesized using the unique RES-C method were demonstrated. The process, in which the catalytic particles and the support are generated simultaneously, leads to the production of Nanorafts of platinum, no greater than 6 atoms in size, on molybdenum carbide. Not only are the particles smaller and of a unique form relative to platinum particles produced using traditional technique, they are also more strongly bound to the support. This suggests that the technique keeps the surface of the support in a truly reduced state during the impregnation with platinum atoms, allowing a truly unique, not oxygen modulated, bond to form between platinum and carbide. It is postulated that the reduced state of the surface is maintained by the large number of radicals produced by the thermal decomposition of the urea in the initial physical mixture, a process occurring concomitant to the decomposition of the molybdenum carbide precursors and the molecular platinum precursors. This stronger metal/surface bond could result in higher durability of the catalyst. Also, the activity of the Nanorafts were compared to commercial Pt based catalysts and exhibited superior performance, with higher mass activity, better kinetics and lower overpotential for ORR. Lastly, a half-cell AST was utilized to investigate the potential for enhanced durability compared to a tradition Pt/C PEMFC catalyst. A significant improvement in durability has been documented here with much lower ECSA loss recorded for identical potential cycling and duration. More work needs to be done in order to understand the source of this dramatic improvement in durability in addition to understanding the source of enhanced activity.

Acknowledgments

We wish to thank the U.S. Department of Energy Fuel Cell Technologies Office and the Israel Ministry of Defense (MAFAT) for providing funding for this work.

References

1. A. Rabis, P. Rodriguez, and T. J. Schmidt, *ACS Catalysis*, **2**, 864 (2012).
2. H. A. Gasteiger and N. M. Markovic, *Science*, **324**, 48 (2009).
3. M. Oezaslan, F. Hasché, and P. Strasser, *The Journal of Physical Chemistry Letters*, **4**, 3273 (2013).
4. C. Wang, N. M. Markovic, and V. R. Stamenkovic, *ACS Catalysis*, **2**, 891 (2012).
5. M. Nesselberger, M. Roefzaad, R. Fayçal Hamou, P. Ulrich Biedermann, F. F. Schweinberger, S. Kunz, K. Schloegl, G. K. H. Wiberg, S. Ashton, U. Heiz, K. J. J. Mayrhofer, and M. Arenz, *Nat Mater*, **12**, 919 (2013).
6. B. Qiao, A. Wang, X. Yang, L. F. Allard, Z. Jiang, Y. Cui, J. Liu, J. Li, and T. Zhang, *Nat Chem*, **3**, 634 (2011).
7. T. Barth and G. Lunde, *Z. physik. Chem.*, **121**, 78 (1926).
8. E. V. Clougherty, K. H. Lothrop, and J. A. Kafalas, *Nature (London, U. K.)*, **191**, 1194 (1961).
9. E. Rudy, S. Windisch, A. J. Stosick, and J. R. Hoffman, *Trans. Metall. Soc. AIME*, **239**, 1247 (1967).
10. G. A. Gruver, *Journal of The Electrochemical Society*, **125**, 1719 (1978).
11. J. P. Meyers and R. M. Darling, *Journal of The Electrochemical Society*, **153**, A1432 (2006).
12. L. T. Weng, P. Bertrand, J. H. Stone-Masui, and W. E. E. Stone, *Surf. Interface Anal.*, **21**, 387 (1994).
13. K. J. Armstrong, L. Elbaz, E. Bauer, A. K. Burrell, T. M. McCleskey, and E. L. Brosha, *J. Mater. Res.*, **27**, 2046 (2012).
14. K. J. Blackmore, L. Elbaz, E. Bauer, E. L. Brosha, K. More, T. M. McCleskey, and A. K. Burrell, *J. Electrochem. Soc.*, **158**, B1255 (2011).
15. Q. Ouyang, H. Li, Z. Zheng, and L. Weng, *Hua Xi Yi Ke Da Xue Xue Bao*, **25**, 178 (1994).
16. R. Guil-Lopez, M. V. Martinez-Huerta, O. Guillen-Villafuerte, M. A. Pena, J. L. G. Fierro, and E. Pastor, *International Journal of Hydrogen Energy*, **35**, 7881 (2010).
17. L. Z. Zeng, S. F. Zhao, Y. Q. Wang, H. Li, and W. S. Li, *International Journal of Hydrogen Energy*, **37**, 4590 (2012).
18. L. Jian-Hui, F. Xian-Zhu, L. Jing-Li, K. T. Chuang, and A. R. Sanger, *Electrochemistry Communications*, **15**, 81 (2012).
19. K. G. Nishanth, P. Sridhar, S. Pitchumani, and A. K. Shukla, *Fuel Cells*, **12**, 146 (2012).
20. A. M. Alexander and J. S. Hargreaves, *Chem Soc Rev*, **39**, 4388 (2010).
21. K. Page, J. Li, R. Savinelli, H. N. Szumila, J. Zhang, J. K. Stalick, T. Proffen, S. L. Scott, and R. Seshadri, *Solid State Sciences*, **10**, 1499 (2008).
22. S. T. Oyama, *Catalysis Today*, **15**, 179 (1992).
23. S. Li, W. B. Kim, and J. S. Lee, *Chemistry Materials*, **10**, 1853 (1998).
24. L. Elbaz, C. Kreller, N. Henson, and E. L. Brosha, *Journal of Electroanalytical Chemistry*, **34**, 720 (2014).
25. Q. X. Jia, T. M. McCleskey, A. K. Burrell, Y. Lin, G. E. Collis, H. Wang, A. D. Q. Li, and S. R. Foltyn, *Nat Mater*, **3**, 529 (2004).
26. Y. M. Shulga, A. V. Bulatov, R. A. T. Gould, W. V. Konze, and L. H. Pignolet, *Inorganic Chemistry*, **31**, 4704 (1992).
27. A. Patel, K. Artyushkova, P. Atanassov, V. Colbow, M. Dutta, D. Harvey, and S. Wessel, *Journal of Vacuum Science & Technology A*, **30** (2012).
28. M. T. M. Koper and I. Wiley, Wiley: Hoboken, N.J., 2009.
29. C. Song, J. Zhang, and J. In *PEM Fuel Cell Electrocatalysts and Catalyst Layers*; J. Zhang, Ed.; Springer London: 2008, p 89.
30. Y. Shao, J. Wang, R. Kou, M. Engelhard, J. Liu, Y. Wang, and Y. Lin, *Electrochim Acta*, **54**, 3109 (2009).